Tunable Molecular Distortion in a Nickel Complex Coupled to a Reversible Phase Transition in the Crystalline State

Larry R. Falvello,*,† Michael A. Hitchman,*,‡ Fernando Palacio,§ Isabel Pascual,† Arthur J. Schultz,⊥ Horst Stratemeier,‡ Milagros Tomás,† Esteban P. Urriolabeitia,† and Dianna M. Young⊥

Contribution from the Departments of Inorganic Chemistry and Condensed Matter Physics, University of Zaragoza−C.S.I.C., Plaza San Francisco s/n, E-50009 Zaragoza, Spain, Department of Chemistry, University of Tasmania, Box 252-75, Hobart, Tasmania 7001, Australia, and Intense Pulsed Neutron Source, Argonne National Laboratory, Argonne, Illinois 60439-4814

Received September 10, 1998

Abstract: The six-coordinate coordination complex *trans*-[Ni(cyan-κN)$_2$(NH$_3$)$_4$] has been characterized in the solid state by X-ray and neutron diffraction at temperatures ranging from 11 to 298 K, by electronic spectroscopy over the temperature range 14−297 K, and by magnetic susceptibility measurements from 1.8 to 300 K. At room temperature the observed space group is *Fmmm*, although there is reason to believe that at a finer level of distinction it is really *Cmcm* approximating *Fmmm*. The nickel center lies on a site of apparent point symmetry *mmm*. At lower temperatures, the space group is unambiguously *Cmcm* without appreciable change in the unit cell parameters, and the molecule lies at a site of *m2m* symmetry. The shape of the molecule changes smoothly with temperature variations from room temperature down to about 140 K, in a behavior characteristic of second-order phase transformations. The molecular shape varies, but by lesser amounts, below 140 K. Possible causes of this phenomenon are discussed. The increase in intensity on cooling of some of the bands observed in the polarized crystal spectrum of the complex is consistent with the change in the molecular structure. Bonding parameters derived from the transition energies indicate that the cyanurate produces a very weak ligand field, which is consistent with the long metal−ligand bond to this ligand. The magnetic properties of the solid display Curie−Weiss behavior through the temperature range of the most pronounced molecular shape changes, but antiferromagnetic interactions become significant below 50 K, with antiferromagnetic ordering at 2.61 K. The propagation pathways for the magnetic interactions are inferred.

Introduction

Polyfunctional ligands—organic ligands possessing more than one functional group—can be used to prepare molecular materials with considerable stress about transition-metal centers, because the ligands are capable of entering into strong interactions with their crystalline surroundings in addition to their usual function of binding to the transition metal. In the course of our studies with such complexes, we have encountered systems in which the intermolecular interactions are structurally dominant, leading to a nonoptimum stereochemistry about the transition metal, manifest in the form of such phenomena as bent bonding, unusual coordination geometries or stoichiometries, or re-expression of a Jahn−Teller effect from static to dynamic distortion.[1,2] In addition to the interesting structural phenomena themselves that arise with polyfunctional ligands in coordination chemistry, these systems also yield products or phases in which transition-metal centers can be studied spectroscopically or by way of magnetism, in unusual geometries or with unusual coordination modes.

One useful polyfunctional ligand is cyanurate, a planar entity which can exist as either the conjugate base of triazine triol (cyanurate-*O*) or as the triketo tautomer, cyanurate-*N*. We have

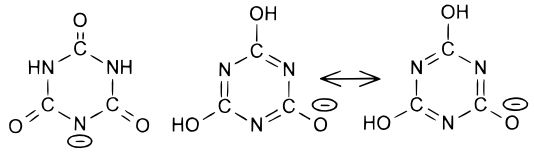

conducted a thorough study of the coordination chemistry of cyanurate-*N*, which is capable of bonding to a metal and, at the same time, of forming an extended, structurally dominant chain involving either free cyanurates or cyanurate ligands of other molecules, or both. The structural dominance of the supramolecular aggregate leads to bent bonding and to odd stoichiometries about the transition metals.[1]

This report concerns the molecular system *trans*-[Ni(cyan-κN)$_2$(NH$_3$)$_4$], which exhibits a striking behavior in the crystalline state. As a coordination complex, *trans*-[Ni(cyan-κN)$_2$(NH$_3$)$_4$] has the expected six-coordinate, octahedral shape and the expected purple color and matching electronic spectrum at room temperature. As with all other cyanurate complexes studied to date, the cyanurate ligands participate in an extended chain formed by hydrogen bonding between ligands of adjacent

† Department of Inorganic Chemistry, University of Zaragoza−C.S.I.C.
‡ University of Tasmania.
§ Department of Condensed Matter Physics, University of Zaragoza−C.S.I.C.
⊥ Argonne National Laboratory.

(1) (a) Falvello, L. R.; Pascual, I.; Tomás, M.; Urriolabeitia, E. P. *J. Am. Chem. Soc.* **1997**, *119*, 11894−11902. (b) Falvello, L. R.; Pascual, I.; Tomás, M. *Inorg. Chim. Acta* **1995**, *229*, 135−142.

(2) Cotton, F. A.; Falvello, L. R.; Ohlhausen, E. L.; Murillo, C. A.; Quesada, J. F. *Z. Anorg. Allg. Chem.* **1991**, *598/599*, 53−70.

10.1021/ja983247t CCC: $18.00
Published on Web 03/16/1999

Table 1. Crystal Data for *trans*-[Ni(cyan-κN)$_2$(NH$_3$)$_4$], from the X-ray Analyses

determination	1a	1b	1c	2a	2b	2c	3	4
temperature, K	298	150	100	298	139	298	223	148
space group[a]	*Cmcm*/*Fmmm*	*Cmcm*	*Cmcm*	*Cmcm*/*Fmmm*	*Cmcm*	*Cmcm*/*Fmmm*	*Cmcm*	*Cmcm*
formula	$C_6H_{16}N_{10}NiO_6$							
fw	382.95							
crystal system	orthorhombic							
crystal color	purple/violet							
a, Å	12.0455(12)	12.014(2)	11.998(4)	12.0551(6)	12.015(2)	12.0551(12)	12.0338(11)	12.006(2)
b, Å	7.2710(12)	7.219(2)	7.203(6)	7.2825(6)	7.226(2)	7.2846(12)	7.2535(10)	7.215(2)
c, Å	16.0707(15)	15.805(2)	15.736(5)	16.0779(7)	15.766(3)	16.0766(14)	15.9377(13)	15.809(3)
V, Å^3	1407.5(3)	1370.7(5)	1359.9(13)	1411.5(2)	1368.7(6)	1411.8(3)	1391.2(3)	1369.4(5)
Z	4							
radiation	Mo Kα ($\lambda_{\langle\alpha\rangle}$ = 0.710 73 Å) (graphite monochromated)							
2θ (min,max), deg	4.0−50.0	4.0−50.0	4.0−60.0	4.0−60.0	4.0−60.0	4.0−60.0	4.0−60.0	4.0−50.0
no. of unique data	370	666	1068	595	1067	597	1094	667
no. of data with $F \geq 2\sigma(F)$	321	565	871	483	880	486	942	511
no., type of data in refinement	370 F_o^2	613 F_o^2	1032 F_o^2	544 F_o^2	1067 F_o^2	597 F_o^2	1094 F_o^2	667 F_o^2
no. of parameters refined	49	80	80	49	80	49	72	80
w$R2$[b]	0.1057	0.0943	0.0951	0.0951	0.0859	0.0827	0.0895	0.1020
$R1$[c] (for $F_o^2 \geq 2\sigma(F_o^2)$)	0.0398	0.0371	0.0393	0.0382	0.0334	0.0301	0.0313	0.0434
quality of fit[d]	1.076	1.096	1.069	1.087	0.997	1.075	1.120	1.033
mean, max $\lvert\Delta/\sigma\rvert$	<0.001, 0.002	<0.001, <0.001	<0.001, 0.001	<0.001, <0.001	0.001, 0.008	<0.001, 0.001	0.003, 0.017	0.002, 0.009
max,min $\Delta\rho$, e/Å^3	0.47,−0.31	0.59,−0.36	0.98,−0.50	0.38,−0.27	0.42,−0.41	0.40,−0.24	0.81,−0.44	0.71,−0.48

[a] See the text for a description of the space group ambiguity in the structures at T = 298 K. [b] w$R2 = [\sum w(F_o^2-F_c^2)^2/\sum w(F_o^2)^2]^{1/2}$. [c] $R1 = \sum||F_{obs}| - |F_{calc}||/\sum|F_{obs}|$. [d] qof $= [\sum w(F_o^2 - F_c^2)^2/(n_{obs} - n_{params})]^{1/2}$.

molecules. The cyanurate ribbons are stacked in the extended crystal structure, with a distance of about 3.5 Å between adjacent ribbons in the stack, as described in a previous report.[1a]

We have now observed that crystals of this molecular material undergo a reversible, nondestructive phase transformation on changing the temperature. The change occurs with a concerted tilting of the stacked cyanurate ribbons and involves a rearrangement of the packing in such a way that neither the cell constants nor the integrity of the crystalline sample is significantly affected. At room temperature the molecule presents a nearly symmetrical appearance, with the nickel atom and the two cyanurate ligands nearly lying in the same plane, so that the coordination symmetry approximates to D_{2h}. In the distorted structure at 100 K, the cyanurate ligands on a given nickel atom are bent out of the coordination plane, making an angle of 33.3° with each other—leading to significantly bent bonding and an overall symmetry of C_{2v} for the coordination about nickel. At intermediate temperatures the distortion of the extended structure, and the concomitant molecular distortion, are intermediate and vary smoothly with temperature, characteristic of a second-order phase transformation. The transformation is reversible and can be recycled after reversal.

The single-crystal electronic spectrum shows the effects of the lowering of the symmetry about the nickel center, and features of the electronic spectrum could, in principle, be used to track temperature changes. In what follows we describe the preparation and characterization of this new thermomorphic molecular material.

Experimental Section

Preparation of *trans*-[Ni(cyan-κN)$_2$(NH$_3$)$_4$]. Infrared spectra of freshly prepared samples were recorded in the range 4000−200 cm^{-1} on Perkin-Elmer 883 and FT1730 spectrophotometers, using Nujol mulls mounted between polystyrene films. Elemental analyses (C,H,N) were performed on a Perkin-Elmer model 240B microanalyzer. Cyanuric acid was purchased from Aldrich and used without further purification. $NiBr_2$ was purchased from Merck.

The preparation of *trans*-[Ni(cyan-κN)$_2$(NH$_3$)$_4$] has been reported before[1a] and is repeated here for convenience. $NiBr_2$ (0.2 g, 0.9 mmol) and Hcyan (0.24 g, 1.8 mmol) were dissolved in boiling water (30 mL). To the hot stirring solution was added 4 mL of concentrated aqueous NH_4OH (28% NH_3 by weight). The solution turned blue-violet, and a violet solid precipitated after 2 days at 3 °C. After the initial precipitate had been filtered, violet crystals were obtained from the mother liquor after it had been kept at 3 °C for 1 week. Yield: 0.15 g (43%). Anal. Calcd for $C_6H_{16}N_{10}NiO_6$: C, 18.82; H, 4.21; N, 36.58. Found: C, 18.90; H, 4.05; N, 36.31. IR (cm^{-1}): 3396 (m), 3150 (s), 1773 (m), 1723 (s), 1682−1409 (vs), 1372 (vs), 1137 (s), 834 (m), 550 (s), 467 (m), 422 (m).

Preparation of Crystals of *trans*-[Ni(cyan-κN)$_2$(NH$_3$)$_4$] for X-ray and Neutron Diffraction Studies and for Single-Crystal Electronic Spectroscopy. Large, regular violet crystals can be obtained from the mother liquor upon cooling. In a typical preparation, the boiling filtrate from the synthesis was rapidly cooled to room temperature in order to precipitate all of the unreacted ligand, which was then filtered off. The deep-violet supernatant solution was stored in a closed vessel at room temperature for 2 weeks and then at +3 °C for another 2 weeks, yielding a crop of large crystals.

Characterization by X-ray Diffraction at Temperatures from 100 to 298 K. Single-crystal X-ray diffraction measurements were made on a Nonius CAD-4 four-circle diffractometer equipped with Mo Kα radiation.[3] Temperature control was effected by a Nonius FR558SH temperature controller, which uses a coaxial pair of nitrogen gas streams for sample temperature adjustment.

X-ray diffraction data were measured from four crystals at a total of six temperatures. A fifth crystal was measured at a single temperature by neutron diffraction (see below). A summary of the X-ray diffraction experiments is given in Table 1. Crystal **1** was measured at three temperatures—298, 150, and 100 K—and revealed the phase transition. Crystal **2** was used to test the reversibility of the transition; this crystal was measured first at a controlled temperature of 298 K, and then at 139 K, and then again at 298 K. The temperature changes between the first and second data sets and between the second and third were conducted in a controlled fashion, and the diffraction properties of the

(3) Diffractometer control program: CAD4/PC Version 1.5c, 1994, and Version 2.0, 1996, Nonius bv, Delft, The Netherlands.

crystal were followed during the transitions. First, while passing from 298 to 139 K, the temperature was lowered in increments of 15 K. At each temperature the crystal was allowed to sit for 15 min, and then a 15-min normal-beam oscillation photograph was taken for the axis [011]; this axis has twice the spacing in the low-temperature *C*-centered phase as it does in the room-temperature *F*-centered phase. Following the photograph at each temperature, the profiles of 12 reflections of varying intensity—eight of which were systematic absences in the *F*-centered phase but not in the *C*-centered phase and four of which were present in both phases—were measured. This procedure was intended to give both a visual and a more rigorous numerical description of the evolution of the crystal with temperature.

The same procedure was used when the temperature was raised again following data collection at 139 K. After the temperature had been raised back to 298 K, the structure was determined once more at this temperature for comparison with the original 298 K determination. To fill in geometric data at an intermediate temperature, the structure was determined independently at 223 K from a third crystal, **3**. A further determination was made at 148 K from crystal **4**.

Measured absorption corrections were applied to each data set.[4] Each structure was solved and refined independently.[5] Coordinates from one determination were not used in any case as the starting point for another. The structures were refined with the programs SHELXL-93 and SHELXL-97.[6] For each determination, all measured reflections that were not systematic absences in the space group employed were used in the refinement, and the structures were refined to F_o^2. The structure at 223 K, **3**, was the only one to receive special treatment. One of the two crystallographically independent ammonia ligands was disordered over two positions related by a rotation about the Ni−N bond. The quality of the data, together with the fact that both congeners are involved in hydrogen bonding, permitted the observation of points corresponding to half occupancy of the hydrogen atom positions. Both congeners were refined as rigid NH_3 groups, each of which was permitted variable rotation about the Ni−N bond. The two congeners represent the two different orientations of this group, namely that found in the room-temperature structure and that found, without disorder, in the rest of the *Cmcm* structures. This point is discussed more fully below.

Because of an ambiguity in the interpretation of the structure at room temperature (to be discussed below), for **1a** all reflections were measured, including those that should be systematically absent in space group *Fmmm*. Of the 1098 systematic absences for *Fmmm*, 18 had intensities *I* just above $3\sigma(I)$. Although there is good reason to give serious consideration to space group *Cmcm* for the 298 K structures, the refinements reported here for **1a**, **2a**, and **2c** were all done with space group *Fmmm*. Special characteristics of these results, and in particular an unusual feature found in the displacement ellipsoids, are described in more detail in the Discussion.

All of our attempts to determine the structure above room temperature, specifically at 333 and 353 K, resulted in failure. Abrupt heating leads to catastrophic breakdown of the sample, while raising the temperature slowly to 333 K leads to severe deterioration of the diffracted peak shapes.

Neutron Structure Determination at 11−16 K. . Neutron diffraction data were taken from a single crystal of *trans*-[Ni(cyan-κN)$_2$(NH_3)$_4$] on the single-crystal diffractometer (SCD) beam line at the Intense Pulsed Neutron Source at Argonne National Laboratory. The SCD instrument is a fixed-detector energy-dispersive instrument with a time- and position-sensitive detector. Neutrons are produced by the pulsed (30 Hz) spallation source at IPNS, and the SCD instrument uses the entire thermal spectrum of neutrons from each pulse. The SCD position-sensitive neutron detector contains a ^{6}Li glass scintillator with dimensions of 30 × 30 cm^2. For a given crystal setting, data are stored in a three-dimensional histogram in which each point has coordinates *x*, *y*, and *t*, which are the horizontal and vertical detector positions and the time-of-flight, respectively. Time-of-flight, *t*, is related to the neutron wavelength λ by the de Broglie equation $\lambda = (h/m)(t/l)$, in which *h* is Planck's constant, *m* is the neutron mass, and *l* is the path length traversed in time *t*. There are 120 time-of-flight channels in each histogram, constructed in such a way that $\Delta t/t$ has a constant value of 0.015. Each histogram comprises measurements of a three-dimensional block of reciprocal space, from neutrons in the wavelength range of 0.7−4.2 Å. A detailed description of the SCD instrument and data collection and analysis procedures has been given in the literature.[7,8] Sample temperature is controlled by a Displex closed-cycle helium refrigerator (Air Products and Chemicals, Inc., model CS-202). Due to a problem with the refrigerator, the sample temperature drifted from 11 to 16 K during the week of data collection.

Table 2. Experimental Parameters from the Neutron Structure Determination of *trans*-[Ni(cyan-κN)$_2$(NH_3)$_4$]

determination	**5**
temperature	11−16 K
pressure	ambient
space group	*Cmcm*
a, Å	12.0323(15)
b, Å	7.2266(12)
c, Å	15.661(6)
V, Å^3	1361.8(6)
Z	4
radiation	neutrons, $\lambda = 0.7-4.2$ Å
data collection technique	TOF Laue with position-sensitive area detector
$\mu(\lambda)$, cm^{-1}	$1.537 + 1.698\cdot\lambda$
no. of reflns in final l s with $F_o^2 > 3\sigma(F_o^2)$	1164
function minimized	$\sum(F_o - F_c)^2$
$R_w(F^2)$	0.091
$R(F^2)$	0.094
$R_w(F)$	0.045
$R(F)$	0.069
GOF	2.86

For the crystal of *trans*-[Ni(cyan-κN)$_2$(NH_3)$_4$], an initial orientation matrix was obtained by an autoindexing algorithm[9] from peaks in one histogram. The occurrence of the *C*-centered phase at the temperature of the experiment was verified. For intensity data collection, 14 histograms were measured—each for a different χ and ϕ crystal setting—in order to cover a unique octant of reciprocal space. Bragg peaks were integrated in three dimensions about their predicted locations and were corrected for the incident neutron spectrum, detector efficiency, and deadtime loss. Lorentz and absorption corrections were also applied. The structure was refined using the program GSAS.[10] In the final least-squares cycle, all atoms including hydrogen atoms were refined with anisotropic temperature factors. A summary of parameters related to the neutron diffraction experiment is presented in Table 2.

Single-Crystal Electronic Spectroscopy. Single-crystal electronic spectra of *trans*-[Ni(cyan-κN)$_2$(NH_3)$_4$] were recorded on a Cary 5A spectrophotometer by the method described previously,[11] with the sample cooled using a Cryodyne model 21 cryostat. The morphology of one of the crystals studied was determined by X-ray diffraction,

(4) Data were processed on an AlphaStation 200 4/166 (OpenVMS/Alpha V6.2), with the program XCAD4B (K. Harms, 1996) and with the commercial package SHELXTL Release 5.05/VMS: 1996, Siemens Analytical X-ray Instruments, Inc., Madison, WI. Processing was also done on a Local Area VAXcluster (VMS V5.5-2) with the commercial package SHELXTL-PLUS Release 4.21/V: 1990, Siemens Analytical X-ray Instruments, Inc., Madison, WI. Further calculations were done on a Hewlett-Packard 9000 model 715/50 (HP-UX V9.05).

(5) SHELXS-86: Fortran program for crystal structure solution, Sheldrick, G. M., University of Göttingen, Germany, 1986.

(6) (a) SHELXL-93: FORTRAN-77 program for the refinement of crystal structures from diffraction data, Sheldrick, G. M., University of Göttingen, Germany, 1993. (b) SHELXL-97: FORTRAN program for crystal structure refinement, Sheldrick, G. M., 1997.

(7) Schultz, A. J.; Van Derveer, D. G.; Parker, D. W.; Baldwin, J. E. *Acta Crystallogr., Sect. C* **1990**, *C46*, 276−279.

(8) Schultz, A. J. *Trans. Am. Crystallogr. Assoc.* **1987**, *23*, 61−69.

(9) Jacobson, R. A. *J. Appl. Crystallogr.* **1986**, *19*, 283−286.

(10) Larson, A. C.; Von Dreele, R. B. *General Structure Analysis System−GSAS*, Report LA-UR 86-748; Los Alamos National Laboratory: Los Alamos, NM, 1994.

(11) Hitchman, M. A.; Riley, M. J. Polarized Absorption Spectroscopy. In *Inorganic Electronic Structure and Spectroscopy*, Vol. 1; Lever, A. B. P., Solomon, E. I., Eds.; Wiley: New York, in press.

Table 3. Molecular Shape Parameters for *trans*-[Ni(cyan-κN)$_2$(NH$_3$)$_4$]

determination	1a	1b	1c	2a	2b	2c	3	4	5
temperature, K	298	150	100	298	139	298	223	148	13
space group[a]	*Cmcm*/*Fmmm*	*Cmcm*	*Cmcm*	*Cmcm*/*Fmmm*	*Cmcm*	*Cmcm*/*Fmmm*	*Cmcm*	*Cmcm*	*Cmcm*
ang distortion param, deg	0	12.1	13.6	0	13.2	0	8.7	12.0	15.3
dihedral, deg[b]	0	29.55(8)	33.28(8)	0	32.14(5)	0	21.61(4)	29.48(10)	35.18(1)
Ni−N(1), Å	2.295(5)	2.270(4)	2.260(3)	2.293(3)	2.265(2)	2.297(2)	2.280(2)	2.268(4)	2.257(3)
Ni−N(2) (T = 298 K), Å	2.068(5)			2.068(3)		2.066(2)			
Ni−N(4) (*Cmcm*), Å		2.072(5)	2.073(3)		2.079(2)		2.074(2)	2.069(6)	2.087(2)
Ni−N(5) (*Cmcm*), Å		2.060(4)	2.065(3)		2.066(2)		2.063(2)	2.061(6)	2.075(2)
N(2)···O(4′) (T = 298 K), Å[c]	3.095(5)			3.107(3)		3.111(3)	3.061(3)		
H(20)···O(4′), Å	2.37(6)			2.55(5)		2.50(4)	2.39		
N(2)−H(20)···O(4′), deg	131(3)			133(3)		132(2)	133		
N(4)···O(4′) (*Cmcm*), Å[d]		3.029(6)	3.021(3)		3.027(3)		3.061(3)	3.035(7)	3.013(4)
H(41)···O(4′), Å		2.26(7)	2.32(4)		2.30(4)		2.30	2.25(6)	2.137(6)
N(4)−H(41)···O(4′), deg		157(5)	147(3)		147(3)		144	156(5)	144.9(4)
N(5)···O(4″), Å[e]		3.160(5)	3.165(4)		3.165(3)		3.140(3)	3.141(7)	3.189(4)
H(52)···O(4″), Å		2.47(6)	2.51(5)		2.54(4)		2.49(3)	2.49(7)	2.442(5)
N(5)−H(52)···O(4″), deg		134(2)	135(1)		133(2)		135(1)	132(3)	130.7(2)
cyan stacking distance 1, Å[f]	3.6355(6)	3.586(17)	3.547(13)	3.6413(3)	3.566(10)	3.6423(6)	3.649(10)	3.58(2)	3.493
cyan slip distance 1, Å	0.672	1.632	1.76	0.668	1.72	0.668	1.374	1.63	1.924
cyan stacking distance 2, Å[g]		3.394(19)	3.354(13)		3.378(11)		3.476(11)	3.40(2)	3.330
cyan slip distance 2, Å		0.22	0.31		0.27		0.0	0.21	0.46

[a] See the text for a description of the space group ambiguity for the structures at T = 298 K. [b] Dihedral angle between the six-membered rings of the two cyanurate ligands. [c] O(4′) is at $(x, 0.5 + y, 0.5 + z)$. For structure **3**, with one disordered ammine ligand, this entry describes the interaction N(4)−H(42F)···O(4′), with O(4′) at $(1 - x, 1 - y, 1 - z)$. [d] O(4′) is at $(1 - x,1 - y,1 - z)$. For structure **3**, with the disordered ammine, this entry describes the interaction N(4)−H(41C)···O(4′). [e] O(4″) has coordinates $(1 - x,-y,1 - z)$. [f] Between the cyanurate at (x,y,z) and that at $(1 - x,1 - y,1 - z)$. [g] Between the cyanurate at (x,y,z) and that at $(1 - x,-y,1 - z)$.

and molar extinction coefficients were obtained by measuring the thickness of this crystal using a microscope.

Bulk Magnetic Measurements. The experiments were performed on a powder sample of *trans*-[Ni(cyan-κN)$_2$(NH$_3$)$_4$] using a SQUID magnetometer manufactured by Quantum Design. The dc susceptibility measurements were made in the temperature range of 1.8 −300 K using a magnetic field of 10 kOe provided by a superconducting magnet. In addition, two magnetization measurements as a function of the magnetic field were made at temperatures of 1.8 and 3.0 K in a field range of up to 50 kOe.

Results

Crystallographic Results. The most important result that emerges from this study is the presence of a temperature-tunable molecular distortion in the complex *trans*-[Ni(cyan-κN)$_2$(NH$_3$)$_4$]. The molecule changes shape in the solid state when its temperature is altered from about 140 to about 300 K. At room temperature, the space group is ambiguous (vide infra) and will be described here as *Cmcm* approximating *Fmmm*, and the positional parameters of the complex conform to the point group D_{2h}, with the resulting mean positions of the atoms of the cyanurate ligands lying in the same plane. However, this is only the *apparent* molecular symmetry derived from X-ray diffraction at room temperature. As will be described more fully in the Discussion, it appears likely that the cyanurate groups in each *trans*-[Ni(cyan-κN)$_2$(NH$_3$)$_4$] complex tilt slightly in the manner observed in the low-temperature structure, so that the *local* symmetry is C_{2v} in the high-temperature modification. At lower temperatures, a clear tilt is adopted by the ligands, and the space group of the crystal is unambiguously *Cmcm*. With the cyanurate ligands pitched out of a central plane in this manner, the point group of the complex is C_{2v}. Furthermore, the *Cmcm*/C_{2v} structure undergoes progressive distortion as the temperature is lowered.

The bond distances and angles about the nickel center, as determined by X-ray and neutron diffraction, show no unusual features and do not vary significantly with changes in temperature. The more important distances and angles are collected in Table 3 for all of the present determinations of the structure.

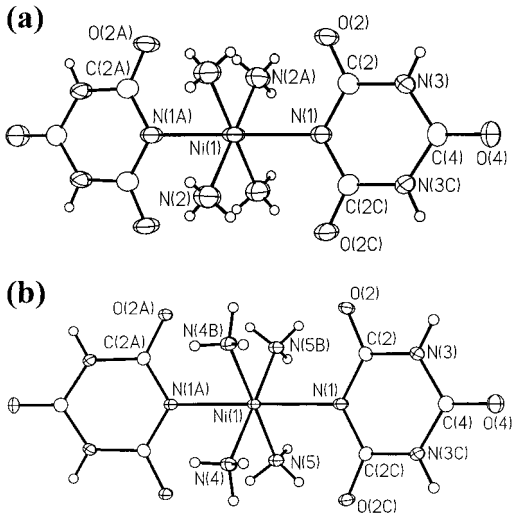

Figure 1. Thermal ellipsoid plots showing the atom naming scheme for *trans*-[Ni(cyan-κN)$_2$(NH$_3$)$_4$] (a) in the structure at 298 K, with data taken from **2a**, and (b) in the *Cmcm* structure, with data taken from **2b**. Non-hydrogen atoms are represented by their 50% probability ellipsoids. Atoms with "A", "B", or "C" appended to their names are symmetry relatives of the corresponding atoms with unmodified names.

The Ni−N bond distances show no important variations with temperature, although the Ni−N(cyan) distance, Ni(1)−N(1), is systematically, albeit very slightly, shorter in the low-temperature *Cmcm* phase. In both phases, the bond length to the cyanurate is significantly longer than that to the ammonia groups (∼2.28 compared with ∼2.07 Å). Figure 1a shows a view of one molecule of *trans*-[Ni(cyan-κN)$_2$(NH$_3$)$_4$], showing the atom labeling scheme used for the room-temperature structure refined with *Fmmm*, in which the asymmetric unit consists of one-eighth of a molecule; Figure 1b shows the atom labeling scheme used for all of the distorted *Cmcm* structures, with a quarter of a molecule in the crystallographic asymmetric unit.

With respect to the progressive pitching of the cyanurates with lowering temperature, shown in Figure 2, we can refer to

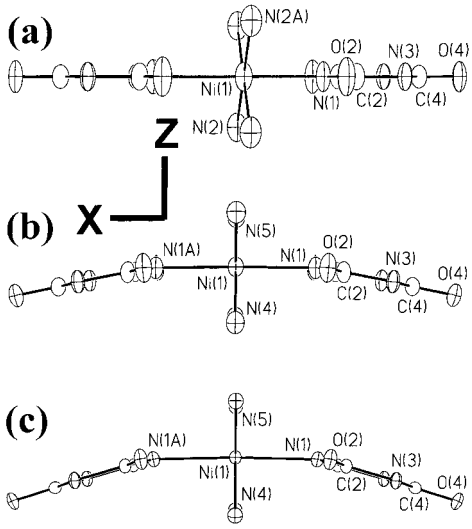

Figure 2. Lateral view of one molecule of *trans*-[Ni(cyan-κN)$_2$(NH$_3$)$_4$] at various temperatures, showing the changing dihedral angle between the cyanurate groups. (a) **2a**, 298 K, dihedral angle = 0°. (b) **3**, 223 K, dihedral = 21.61(4)°. (c) **2b**, 139 K, dihedral = 32.14(5)°. Hydrogen atoms are not shown. Non-hydrogen atoms are represented by their 50% probability ellipsoids. Structures **2a** (a) and **2b** (c) are from the same crystal. The directions (*X*,*Z*) shown refer to the reference frame used for the spectroscopic study, for which *Y* is the direction perpendicular to these drawings.

two parameters in order to quantify the molecular distortion. The first is the dihedral angle between the planes of the two cyanurate ligands of a given molecule. The side-on views shown in Figure 2 reveal the progressive shape change. The second useful indicator for the molecular shape change is an angular distortion parameter more closely related to bonding concepts, which we shall define as the angle between the Ni(1)−N(1) bond and the external bisector of the angle C(2)−N(1)−C(2C). This entity has traditionally been called a misdirected valence parameter, but in the present case the question of misdirected valence is somewhat more complex because of the possibility of rehybridization at the bound imidate nitrogen atom. This aspect is discussed further in connection with the bonding parameters derived for the complex. Values of the two distortion parameters are listed in Table 3, and these show that the distortion progresses monotonically from room temperature down to about 140 K and then continues much more slowly—almost negligibly—with further lowering of the temperature.

The extended crystal structure, which was described more fully in a previous report, has two principal features. The first is the presence of an unbounded one-dimensional ribbon of cyanurates, which, as has been previously described,[1a] is a persistent aggregate structure in coordination complexes containing cyanurate. The second important feature of the extended structure, one which is involved in the phase transition, is the pattern of intermolecular interactions around a void bounded by parts of the peripheries of four different molecules. It turns out that the change from the room-temperature, "*Cmcm* approximating *Fmmm*" structure to the low-temperature *Cmcm* structure involves a single modification of the hydrogen-bonding pattern. This change is best understood with reference to Figure 3, which shows parts of four molecules of the nickel complex that meet at this junction with weak hydrogen bond interactions among them. In Figure 3a, from the room-temperature structure, the four ammine groups shown—two are shown from each of two different molecules—are all equivalent by crystallographic symmetry in *Fmmm*, the group used for the refinement. Three mirror planes are present—one is the plane of the cyanurate

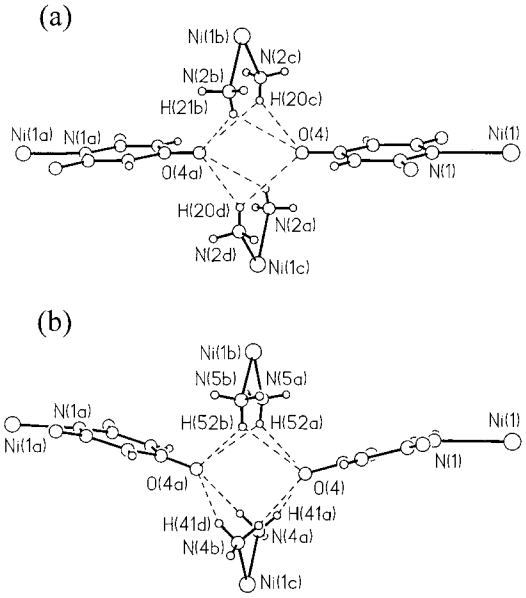

Figure 3. Views of the four-molecule junction in the crystal structure of *trans*-[Ni(cyan-κN)$_2$(NH$_3$)$_4$] (a) at 298 K, **2a**, and (b) at 139 K, **2b**.

ligands, another is the plane containing the four NH$_3$ moieties, and the third contains all four of the nickel atoms shown in Figure 3a and bisects the cyanurate groups as well as the N−Ni−N angles shown in the figure, such as N(2b)−Ni(1b)−N(2c). All of the ammine groups lie in the second crystallographic mirror plane, and the hydrogen atoms that lie in the mirror (H(20c), H(20d), and their unlabeled symmetry relatives) serve as donors in bifurcated hydrogen bonds. The acceptors are *para*-carbonyl oxygen atoms, O(4) and O(4a) of cyanurate ligands from two different molecules. These hydrogen bonds, which are all equivalent to each other by crystallographic symmetry, are weak, with N···O distances of the order of 3.1 Å and N−H···O angles of about 133°. (See Table 3 for the values of N(2)···O(4′), H(20)···O(4′), and N(2)−H(20)···O(4′) from the three determinations of the room-temperature structure.) These values are typical of bifurcated hydrogen bonds.

Upon lowering the temperature, the space group is clearly *Cmcm*, and the symmetry at the molecular junction shown in Figure 3 is lowered. As shown in Figure 3b, taken from structure **2b** at 139 K, the two cyanurate groups now are pitched downward so that the symmetry at the junction is C_{2v}. Two crystallographic mirror planes are present—one containing the four ammine nitrogen atoms, N(4a), N(4b), N(5a), and N(5b), and another that contains the four nickel atoms shown and bisects the N−Ni−N angles as before. The crystallographic 2-fold axis runs vertically in the plane of the figure and bisects the N−Ni−N angles. With this reduced symmetry, only pairs of NH$_3$ groups are equivalent rather than all four of those shown. And along with the tilting down of the cyanurate ligands, two of the ammonia groups—those centered on N(4a) and N(4b)—undergo a change of orientation by 60°. Now the hydrogen atom that interacts with the carbonyl oxygen atom O(4) of cyanurate points more directly at the acceptor. With reference to Figure 3b and using the data from structure **2b**, the distance N(4a)···O(4) is 3.027(3) Å, while H(41a)···O(4) = 2.30(4) Å, and the angle N(4a)−H(41a)···O(4) = 147(3)°. This represents a somewhat stronger interaction than that found in the room-temperature structure. The remaining interactions in Figure 3b, for example that involving N(5a) and O(4), are somewhat weakened with respect to the corresponding interactions shown in Figure 3a. So N(5a)···O(4) = 3.165(3) Å, H(52a)···O(4) = 2.54(4) Å, and N(5a)−H(52a)···O(4) = 133(2)°.

In summary, the change of space group from either exactly or approximately *Fmmm* at room temperature to *Cmcm* at lower temperatures involves a concerted tilting of the cyanurate ligands, rotation of half of the ammonia groups by 60°, and a concomitant strengthening of half of the hydrogen-bonding interactions at four-molecule junctions at the expense of the other half. The structure at 223 K has the ammine ligand at N(4) disordered over the two orientations, that found undisordered at room temperature and that found undisordered at lower temperatures. We note here that the other significant hydrogen bonds in this structure, most notably those that bind the cyanurate ribbon, are unaffected by the structural change.

Another structural variation observed between the *Fmmm* and *Cmcm* results, namely a change in the cyanurate stacking pattern, will be described more fully in the Discussion section.

Spectroscopic Results. The electronic spectrum of the (100) face of several single crystals of *trans*-[Ni(cyan-κN)$_2$(NH$_3$)$_4$] was measured over a temperature range with the electric vector of polarized light along the two extinction directions. A coordinate system defined as shown in Figure 2 was used to interpret the spectra. This relates to the molecular geometry of C_{2v} symmetry observed in the low-temperature crystal modification. It should be noted that because the *z*-axis bisects two of the metal−ligand bond directions in this point group, the d-orbitals are defined differently from those of a complex of O_h symmetry. For instance, the half-filled d-orbitals, pointing approximately along the Ni−N bond directions, are d_{yz} and d_{x^2}. With the axes defined in this way, the complex has a ground state of $^3B_2$ symmetry, and the excited states of $^3T_{2g}$ and $^3T_{1g}$ of an octahedral complex split into levels of $^3A_2$, $^3B_1$, and $^3A_1$, and $^3B_2$, $^3B_1$, and $^3A_2$ symmetry, respectively. In this noncentrosymmetric point group, the transitions to levels of $^3A_2$, $^3A_1$, and $^3B_2$ symmetry are allowed by an electric dipole mechanism when the electric vector is parallel to the *x*, *y*, and *z* molecular axes, respectively. A noncentrosymmetric vibration of the appropriate symmetry is available to induce intensity into each transition in every polarization by vibronic coupling.[11] The intensity of a transition which is electronically "allowed" is normally rather insensitive to temperature, while that induced by vibronic coupling generally decreases on cooling. The temperature dependence can, therefore, provide a useful way of distinguishing between bands produced by the two intensity mechanisms, though when the deviation from a centrosymmetric geometry is small, as in the present case, it must be recognized that the intensity produced by each mechanism may be comparable in magnitude. In addition, for the present complex the crystal structures indicate that the deviation from a center of symmetry increases progressively on cooling, so that the intensity induced by the asymmetric distortion should increase as the temperature is lowered.

The crystal packing is such that the molecular axes of all complexes in the unit cell are parallel. When the electric vector is along *b* it is aligned with the ***z*** molecular axis, while when it is along *c* it is parallel to *x*. Typical spectra at various temperatures are shown in Figure 4, and the energies of the band maxima at 14 and 297 K are given in Table 4. Transitions to three levels of $^3A_2$ symmetry occur, and in agreement with this the spectrum in *x* polarization, where such transitions are electronically allowed, is dominated by three peaks which increase significantly in intensity on cooling. In *z* polarization, transitions to only two levels are allowed, those of $^3B_2$ symmetry. This spectrum is dominated by peaks which decrease in intensity substantially on cooling, implying that here intensity is derived largely by vibronic coupling. When taken in conjunction with the ligand field calculations described in the following section, the band assignments given in Table 4 are consistent with the observed spectra. The polarized spectra observed at 14 K are shown in Figure 5 together with the proposed assignments. Here, the intensities are shown as the molar

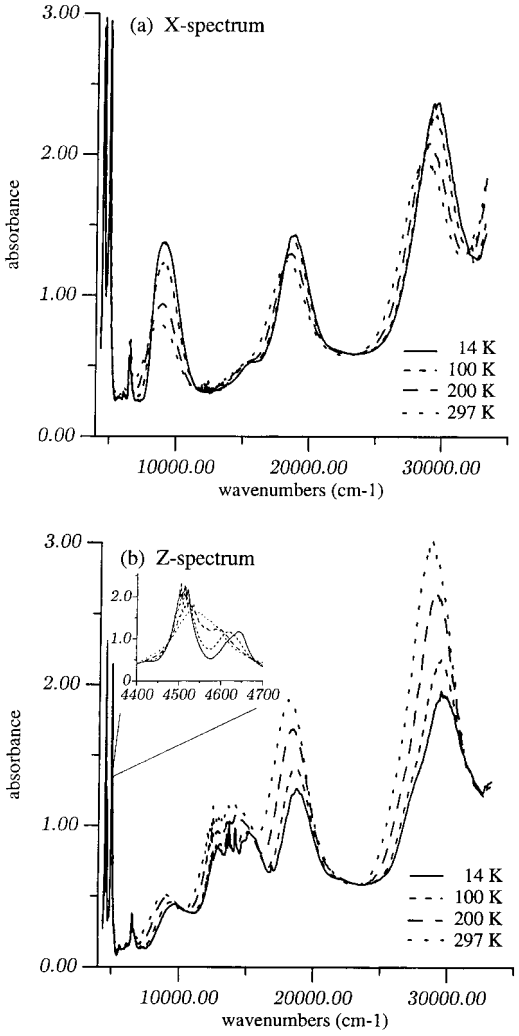

Figure 4. Temperature dependence of the spectrum of the (100) crystal face of *trans*-[Ni(cyan-κN)$_2$(NH$_3$)$_4$] with the electric vector parallel to (a) the *c*-axis and (b) the *b*-axis.

Table 4. Calculated and Observed Transition Energies in cm^{-1} for *trans*-[Ni(cyan-κN)$_2$(NH$_3$)$_4$], Together with the Band Assignments

		observed band maxima			
		$T = 14$ K		$T = 297$ K	
assignments, C_{2v} symmetry	calcd transition energies	$\|\|b$ (z)	$\|\|c$ (x)	$\|\|b$ (z)	$\|\|c$ (x)
$^3B_2 \rightarrow {}^3A_2$	8891		9100		8800
$^3B_1$	8912	9750		8950	
$^3A_1$	13124	12900		12900	
$^1A_1$	13502	13500		13900	
		13700[a]			
		13860[a]			
		14150[a]			
$^1B_2$	15409	15010		14500	
$^3B_2$	15599	15560			
		16900[a]			
$^3B_1$	17951	18700		18150	
$^3A_2$	18498		18800		18400
$^3B_2$	27994	27500			
$^3A_2$	29350	29600	29500	28700	28700
$^3B_1$	29883				

[a] Component of a vibrational progression.

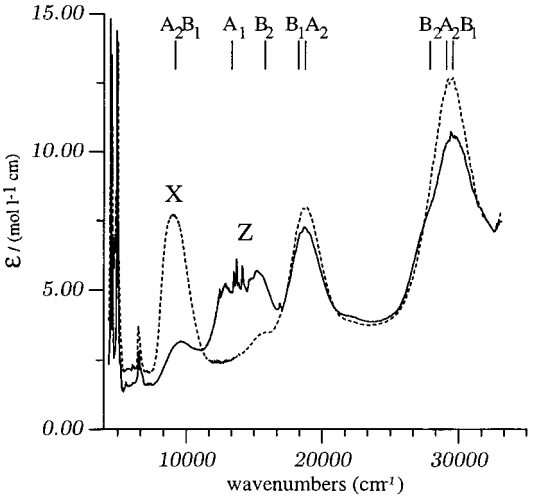

Figure 5. Electronic spectrum of *trans*-[Ni(cyan-κN)$_2$(NH$_3$)$_4$] at 14 K with the electric vector parallel to the *x* and *z* molecular axes. The calculated positions of the spin triplet excited states are indicated above the spectra.

extinction coefficient, and it may be seen that these are quite low, being in the range typically observed for complexes in which the intensity is derived by vibronic coupling or small distortions from a centrosymmetric geometry.[12] The weak sharp peaks at 13 700, 13 860 and 14 150 cm^{-1} are assigned as components of vibronic progressions associated with the spin-forbidden transition to the ^{1}A$_1$ component of the ^{1}E$_g$ level of the parent octahedral complex, at 13 500 cm^{-1}. The transition to the second component, of ^{1}B$_2$ symmetry, is calculated to lie very close to the spin-allowed ^{3}B$_2$ → ^{3}B$_2$ transition. Transitions to both levels presumably contribute to the multiple peaks at ∼14 640, 15 020 and 15 560 cm^{-1}, the remaining peak probably being due to a component of a vibrational progression. The very weak peak at 16 900 cm^{-1} is probably due to coupling of the ^{1}A$_1$ state with an NH stretching vibration of the ammonia ligands; transitions of this type have been reported in the low-temperature spectra of other Ni^{2+} ammine complexes.[13] The peak centered at ∼18 700 cm^{-1} shows evidence of a poorly defined vibrational progression in *z* polarization, with an energy interval of ∼395 cm^{-1}. This is probably due to a vibrational progression in a totally symmetric mode; similar structure involving a progressional interval of 330 ± 20 cm^{-1} was observed on the ^{3}A$_{2g}$ → ^{3}T$_{1g}$(F) transition of Ni(NH$_3$)$_6$(ClO$_4$)$_2$.[13]

The fact that the bands due to the ^{3}B$_2$ → ^{3}A$_2$ transitions increase in intensity on cooling provides strong evidence that the planes of the cyanurate groups do, indeed, tilt progressively as the temperature is lowered. It is possible that in the crystal structure at or just below room temperature, two molecular conformers exist in the *Cmcm* phase, with identical geometries involving tilted cyanurate groups, but with an opposite sense of tilt. If these differed in energy by a small amount, their relative proportion would vary with temperature, so that the *average* tilt observed by X-ray diffraction would be temperature dependent. (We do not have unresolved conformers at any of the temperatures for which data were taken on the unambiguous *Cmcm* structure; in the least distorted of our low-temperature structures, namely **3** which was measured at 223 K, the distance between the *para*-oxygen atom O(4) and a hypothetical congener related by equal and opposite distortion would be 0.84 Å, which would render the two congeners resolvable into separate atomic sites with partial occupancy.) Such behavior, though involving metal−ligand bond lengths, rather than an angular distortion, has often been observed for Cu^{2+} complexes.[14−16] However, since the intensity of an electronic transition depends on the *local* geometry of the complex, rather than its *average* geometry, behavior of this kind would not influence the band intensites. It is interesting to note that intensification of the bands on cooling continues even below the temperature at which the molecular structure reaches its limiting value, ∼140 K (Figure 4). The reason for this is not clear, though the diffraction results do indicate a continuing albeit attenuated distortion at lower temperatures. Further evidence for a true change in molecular geometry of the complex is provided by the infrared combination bands observed in *z* polarization (inset to Figure 4b). A single broad asymmetric band is observed at 297 K, which progressively splits in two on cooling to below 200 K. This presumably reflects the changes in hydrogen bonding which accompany the tilting of the cyanurate ligands.

The spectrum measured at 297 K is that of the crystal in its high-temperature phase (space group *Fmmm*, either rigorous or approximate; note that the extinction directions of the crystal face are unaltered by the phase transition). However, the spectrum differs very little from that of the *Cmcm* phase at high temperature (Figure 4). This supports the conjecture, based upon the high out-of-plane thermal ellipsoid parameters of the atoms in the cyanurate group, that although these ligands are constrained by symmetry to be coplanar when the space group *Fmmm* is used for refinement, the *local* symmetry of the *trans*-[Ni(cyan-κN)$_2$(NH$_3$)$_4$] molecule is C_{2v} in the high-temperature as well as the low-temperature phase (see Discussion, below). The D_{2h} molecular symmetry required for the atomic positions by the space group *Fmmm* thus results either from unresolvable disorder of the tilted cyanarate groups or simply from the fact that a structure deviating slightly from *Fmmm* symmetry was constrained to conform to it. Since it is the local symmetry which decides the mechanism by which the "d−d" transitions gain intensity, the C_{2v} selection rules are therefore appropriate for the interpretation of the spectrum of both phases of the compound.

Metal−Ligand Bonding Parameters. The transition energies observed for *trans*-[Ni(cyan-κN)$_2$(NH$_3$)$_4$] were used to estimate angular overlap[17] metal−ligand bonding parameters using the computer program AOMX developed by Adamsky.[18] This uses the molecular geometry indicated by the crystal structure and allows "best-fit" bonding parameters to be derived. Initially this was done for the spectra observed at low temperature using the ^{3}B$_2$ → ^{3}A$_2$ transition energies assigned as described above, and with the σ-bonding parameter for the ammonia ligands fixed at the value e_σ(NH$_3$) = 3900 cm^{-1} derived[19] for this ligand in Ni(NH$_3$)$_4$(NO$_2$)$_2$. The assignments this suggested for all the peaks in the spectrum were then included in the derivation of best-fit bonding parameters for both ligands. As in other studies,[12] it was assumed here that the π-bonding interaction

(12) Lever, A. B. P. *Inorganic Electronic Spectroscopy*, 2nd ed.; Elsevier: Amsterdam, 1984.
(13) Shriver, A. F.; Hamm, D. J. *Inorg. Chem.* **1973**, *12*, 2037−2048.
(14) Ammeter, J. H.; Bürgi, H.-B.; Gamp, E.; Meyer-Sandrin, V.; Jensen, W. P. *Inorg. Chem.* **1979**, *18*, 733−750.
(15) Simmons, C. J. *New. J. Chem.* **1993**, *17*, 77−95.
(16) Simmons, C. J.; Hathaway, B. J.; Amornjarusiri, K.; Santarsiero, B. D.; Clearfield, A. *J. Am. Chem. Soc.* **1987**, *109*, 1947−1958.
(17) The basic formulation of the angular overlap model is set out in the following: Schäffer C. E.; Jørgensen, C. K. *Mol. Phys.* **1965**, *9*, 401−412. Recent developments in the model are outlined in the following: Schönherr, T. *Top. Curr. Chem.* **1997**, *191*, 88−152.
(18) The computer program AOMX developed by Dr. H. Adamsky and his colleagues is available on the Internet at http://www.theochem.uni-duesseldorf.de/∼heribert/aomx/aomxhtml/aomxhtml.html.
(19) Hitchman, M. A.; Rowbottom, G. L. *Inorg. Chem.* **1982**, *21*, 823−825.

of the ammonia and the in-plane π-interaction of the cyanurate were both negligible. The effects of both band polarization and temperature were then explored, and it was found that these had little influence upon the best-fit bonding parameters. In particular, raising the temperature from 14 to 297 K produces shifts to lower energy of no more than a few hundred cm^{-1}. Such "red-shifts" are commonly observed for compounds which undergo no structural change and may be explained in terms of changes in the populations of the vibrational levels of the complex.[11,12] This suggests that the bonding parameters do not alter significantly as a function of temperature, and indeed, as shown in Table 4, the transition energies observed at high and low temperature may be reproduced satisfactorily using the set of bonding parameters:

$$e_\sigma(NH_3) = 4395\ cm^{-1}, \quad e_\sigma(\text{cyanurate}) = 1815\ cm^{-1}$$

$$e_\pi(\text{cyanurate}) = 0\ cm^{-1}$$

A Racah parameter $B = 962\ cm^{-1}$ was used in the calculation, which represents a modest reduction from the free ion value of 1041 cm^{-1},[12] and the ratio C/B was taken to be 4.265. Spin−orbit coupling was neglected in the calculation. A calculation was also carried out including this effect using an effective spin−orbit coupling coefficient $\zeta = 450\ cm^{-1}$. Apart from splitting many of the excited levels, this caused a modest zero-field splitting of the ground state, producing upper levels 4.9 and 5.6 cm^{-1} above the lowest state.

The bonding parameter derived for the ammonia groups is somewhat higher than that in other Ni^{2+} ammine complexes.[12,13,19] However, this may be explained by the rather short bond lengths to this ligand in *trans*-[Ni(cyan-κN)$_2$(NH_3)$_4$], ~2.07 Å. Both theory[20] and experiment[21] suggest that metal−ligand bonding parameters vary inversely as about the sixth power of the bond distance, and such a relationship implies a bonding parameter of 3930 cm^{-1} at a bond length equal to that observed for the complex Ni(NH_3)$_4$(NO_2)$_2$, 2.109 Å, which agrees well with the estimate of 3900 cm^{-1} derived for this complex.[19] The σ-bonding parameter of the cyanurate group is less than half that of the ammonia ligand, being in fact similar to the value $e_\sigma = 2000\ cm^{-1}$ reported[22] for the iodide ion bonded to Ni^{2+}. The low value largely reflects the fact that the Ni−N(cyanurate) bonds are much longer than those to ammonia, ~2.296 Å at room temperature and ~2.260 Å at 100 K. Normally, heterocyclic amines have bond lengths which are similar to those typical of ammonia. For instance, the Ni−N distance in the complex ion Ni[(pyrazole)$_3$CH]$_2^{2+}$ is ~2.08 Å.[23] Applying the above correction for distance implies a bonding parameter $e_\sigma \approx 3275\ cm^{-1}$ for a cyanurate group at such a bond length. While this is less than the value of $e_\sigma \approx 4700\ cm^{-1}$ derived for Ni[(pyrazole)$_3$CH]$_2^{2+}$,[23] it suggests that the main cause of the very low σ-bonding parameter of the cyanurate ligands in *trans*-[Ni(cyan-κN)$_2$(NH_3)$_4$] is the length of the metal−ligand bonds. Within the uncertainty limits of the parameters, which is ~200 cm^{-1}, the π-bonding interaction due to the cyanurate ligand is negligable, i.e., $e_\pi \approx 0\ cm^{-1}$. This may also be associated with the long bond length to this ligand, as the π-interaction is expected to be more sensitive to bond distance than the σ-interaction.[24] Heterocyclic amines are normally weak π-donors toward Ni^{2+}; for instance, $e_\pi \approx 630\ cm^{-1}$ in Ni[(pyrazole)$_3$CH]$_2^{2+}$.[23]

It is interesting that the change in tilt angle that occurs on cooling, which causes an increase in intensity of the $^3B_2 \rightarrow {}^3A_2$ transition, has no significant effect on the transition energies, and hence the bonding parameters. This is not entirely unexpected, since the change in structure occurs outside the primary coordination sphere. The tilting of the cyanurate ligand might be associated with a change in hybridization of the σ-bonding orbitals of the nitrogen bonded to the metal from sp^2 toward sp^3. While this cannot be ruled out, the driving force for such a change is not apparent, and it seems unlikely. It seems more probable that the tilting is associated with the adoption of a preferred packing arrangement which develops upon cooling. Resistance to such a change is expected to be low, as the cyanurate groups are bonded only weakly to the metal ion (indeed, the very fact that these bonds are so weak implies that intermolecular interactions may play an important role in the overall lattice energy, perhaps at the expence of metal−ligand interactions). If it is supposed that the lone pair of electrons which interacts with the Ni^{2+} remains coplanar with the cyanurate ligand, then the progressive tilting of this ligand which occurs on cooling will lead to the development of "bent bonds" at low temperature. Misdirected valence of this kind may be treated formally within the framework of the angular overlap model by the addition of an extra parameter,[25] but the absence of experimentally observable effects for the present complex means that such a treatment is not warranted. However, an approximate estimate of the likely influence of the effect may be obtained by noting that the σ-interaction along the bond axis will be reduced to $\cos^2 \alpha e_\sigma$, where α is the angle of tilt.[26] At low temperature, the cyanurate groups bend away from the Ni−N bond vectors by 13.6°, meaning that, neglecting any change in the metal−ligand bond distance, the bonding parameter should decrease by ~5.5%. This corresponds to only ~100 cm^{-1} for the bonding parameter $e_\sigma(\text{cyanurate}) = 1815\ cm^{-1}$, well within the experimental uncertainty. Moreover, the metal−ligand bond length shortens slightly on cooling, which would cause the bonding parameter to increase by an amount which is about equal to the decrease associated with the tilting of the ligand. It is therefore apparent that the temperature invariance of the bonding parameters of *trans*-[Ni(cyan-κN)$_2$(NH_3)$_4$] is quite consistent with the change in geometry observed for the complex.

Magnetic Results. The temperature dependence of the dc magnetic susceptibility is shown in Figure 6. The experimental data have not been corrected for the diamagnetic contribution of the molecule since the correction is considerably smaller than the experimental uncertainty. The susceptibility values increase as the temperature decreases until they reach a maximum at about 4.5 K. The shape of the curve indicates that antiferromagnetic ordering arises at $T_N = 2.61$ K, the maximum value of $d\chi/dT$ (see inset in Figure 6).

At temperatures above 50 K, the susceptibility data follow a Curie−Weiss law, with $C = 1.155$ emu·K/mol and $\theta = -4.48$ K. Figure 7 (left *Y*-axis) presents the temperature dependence of the inverse of the experimental susceptibility (full triangles) and the fit to the Curie−Weiss law (solid line). The spin and *g*-factor values can be determined from the Curie constant as *S*

(20) Bermejo, M.; Pueyo, L. *J. Chem. Phys.* **1983**, *78*, 854−857.
(21) Drickamer, H. G. *J. Chem. Phys.* **1967**, *47*, 1880 and references therein.
(22) Gerloch, M.; Hanton, L. R. *Inorg. Chem.* **1981**, *20*, 1046−1050.
(23) Astley, T.; Gulbis, J. M.; Hitchman, M. A.; Tiekink, E. R. T. *J. Chem. Soc., Dalton Trans.* **1993**, 509−515.
(24) Smith, D. W. *J. Chem. Soc. A* **1970**, 1498−1503.
(25) Deeth, R. J.; Duer, M. J.; Gerloch, M. *Inorg. Chem.* **1987**, *26*, 2578−2582.
(26) Comba, P.; Hambley, T. W.; Hitchman, M. A.; Stratemeier, H. *Inorg. Chem.* **1995**, *34*, 3903−3911.

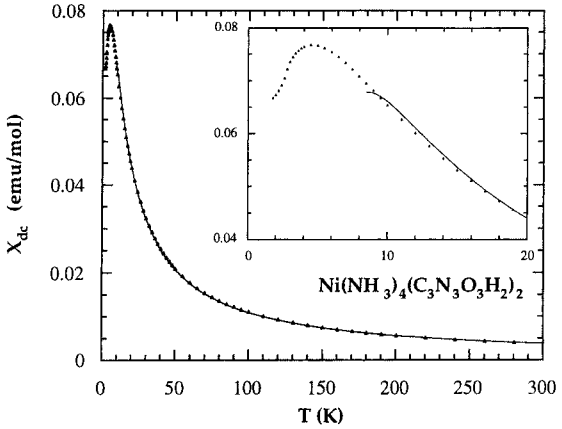

Figure 6. Temperature dependence of the dc magnetic susceptibility of *trans*-[Ni(cyan-κN)$_2$(NH$_3$)$_4$]. The continuous line is the fit of the data to the $S = 1$ square planar Heisenberg model using high-temperature series expansions. The inset shows the low-temperature region in more detail.

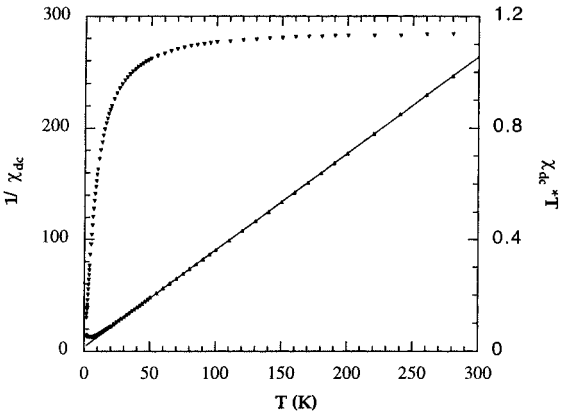

Figure 7. Temperature dependence of the inverse of the magnetic susceptibility of *trans*-[Ni(cyan-κN)$_2$(NH$_3$)$_4$] (left axis) and of χT (right axis). The continuous line is the fit of the data to the Curie−Weiss law.

$= 1$ and $g = 2.15$. These values are consistent with the presence of a Ni^{2+} ion, octahedrally coordinated, as the only magnetic entity in the molecule. No magnetic effects resulting from zero-field splitting (ZFS) are observed above 50 K. In addition, the g-factor has a value rather close to that corresponding to the free electron, and consequently, the ZFS should be expected to be very small—a few degrees at most—in good agreement with the spectroscopic results. The effects of antiferromagnetic interactions can be examined more closely by viewing χT versus T. Although the values of χT are not related to any physical property, in the paramagnetic region they are proportional to the square of the effective magnetic moment and are rather sensitive to its fluctuations. As Figure 7 (right Y-axis) shows, below 50 K the value of χT decreases rapidly as the temperature is lowered. Since a reduction of the effective moment due to ZFS should arise at much lower temperatures, the observed reduction in χT should be attributed to antiferromagnetic interactions between the Ni^{2+} ions.

The magnetization isotherms measured at 1.8 and 3.0 K show a linear dependence on the applied field. A minor change observed at about 30 kOe in the slope of the curve corresponding to the isotherm at 1.8 K might be indicative of a spin−flop transition induced by the applied field. A better understanding of this anomaly would require more detailed measurements taken from single-crystal samples.

Discussion

General Considerations. The coordination compound *trans*-[Ni(cyan-κN)$_2$(NH$_3$)$_4$], in the solid state, changes shape with temperature over the range of about 140−300 K, and the upper limit for the change may even be slightly higher. The molecular shape change is associated with a second-order phase transition in the crystal. The second-order phase transition can be analyzed rigorously, as described in the next section, using any of several order parameters. At the molecular level, the distortion is seen entirely in the angular disposition of the two cyanurate ligands, which have an angular distortion parameter of zero at room temperature and then 8.7° at 223 K, passing on to 13.6° at 100 K. The cyanurate−cyanurate intramolecular dihedral angle varies monotonically from zero at room temperature to 32.14(5)° at 139 K to 33.28(8)° at 100 K (Table 3). Below about 140 K the structural changes are less pronounced.

The nine structure determinations of *trans*-[Ni(cyan-κN)$_2$(NH$_3$)$_4$] presented here are intended to characterize general as well as specific properties of this unusual phenomenon. The cyanurate dihedral angle (Table 3) can serve as a "numerical aphorism" for the structural variation, which can be followed easily in terms of this parameter. The three analyses from crystal 1—**1a** at 298 K, **1b** at 150 K, and **1c** at 100 K—demonstrate the structural change and indicate that its nature is progressive at lower temperatures. The three determinations from crystal 2—**2a** at 298 K, **2b** at 139 K, and **2c** at 298 K—demonstrate the reversibility of the phenomenon. Structure **2c**, which was done after a lengthy series of measurements at temperatures varying in both directions between 298 and 139 K (see Experimental Section), is identical within experimental error to **2a,** which was done at the beginning of the experiment with crystal 2. Between analysis **2a** and analysis **2c**, the crystal had changed from *Fmmm* symmetry (which may be approximate or rigorous) to *Cmcm* and back. Crystal 3, which was analyzed at 223 K, yields an observation of an intermediate level of distortion, establishing that this is a case of a second-order phase transition.[27] Crystal 4, characterized at 148 K, establishes the reproducibility of the results from different crystals. Structure **4** is essentially identical to **1b**, which was measured at 150 K. The neutron structure determination, **5**, at 11−16 K shows that the structure changes to a far lesser extent on proceeding to very low temperature.

In addition to structural characterization, it is possible to follow this phase transformation via the electronic spectrum of the Ni^{2+} ion. The d^8 center is thus a useful probe into the overall shape of the molecule as it is carried through a range of distortion. Conversely, the second-order phase transition offers the rare opportunity to observe a transition−metal center as its ligand field symmetry varies continuously.

Finally, the magnetic experiments permit a deeper characterization of the behavior of the low-temperature structural phase of *trans*-[Ni(cyan-κN)$_2$(NH$_3$)$_4$]. The magnetic ordering of the compound indicates that the interactions between the Ni^{2+} ions extend cooperatively throughout the whole lattice at temperatures below T_N. This permits an analysis of the correlation between the packing of the molecules in the lattice and the propagation pathways of the magnetic interactions.

Nature of the Phase Change. Although we have directed the study of this system more toward its molecular aspects, the solid-state phenomenon involved, namely the phase transition that drives the molecular distortion, is itself worthy of further examination. The phase transition that we observe is principally second order, consisting of a smooth distortion of the crystal

(27) Franzen, H. F. *Physical Chemistry of Inorganic Crystalline Solids*; Springer-Verlag: Berlin, 1986; pp 88−105.

structure as a whole and thus of the molecule of *trans*-[Ni(cyan-κN)$_2$(NH$_3$)$_4$]. From 223 K upward, however, we observe a first-order component, namely a rotation by 60° of half of the ammonia ligands, as they adjust to a more symmetric environment that begins to approach the higher point symmetry D_{2h} at the four-molecule junctions.

A more detailed analysis of the phase transition has been carried out by Bürgi[28] and will be briefly summarized here by way of explaining the space group ambiguity that arises at 298 K. As reviewed by Salje,[29] a second-order, or purely displacive, phase transition that proceeds as some thermodynamic parameter such as temperature is varied involves a change in some structural parameter, the "order parameter", Q, whose variation is related to temperature by eq 1.

$$Q^2 = Q_0^2(1 - T/T_c) \quad (1)$$

Q is any appropriate structural feature, which in this case could be the angular distortion parameter, the dihedral angle between the cyanurates, or the movement of the y-coordinate of the nickel atom. Q_o is the value that this parameter would have at absolute zero temperature if the phase transition continued unabated to that point, and T_c is the "critical temperature", the temperature at which the displacement has a value of zero. In this case, T_c is the upper limit of the transition, the temperature at which the space group becomes unambiguously *Fmmm* and the molecule has rigorous D_{2h} symmetry.

From our structural data it would at first appear that the critical temperature occurs somewhere between 223 and 298 K, since we observe the systematic absences for *F*-centered cells at the latter temperature. However, a plot of Q^2 vs temperature using any of the possible distortion parameters for this structure yields T_c well above 300 K.[30] Specifically, we calculate T_c values of 309, 314, and 315 K using (1) the angular distortion parameter, (2) the dihedral angle between cyanurates, and (3) the shift of the y-coordinate of the nickel atom from a value of 0.25, respectively, as the angular distortion parameter. This would suggest that the space group at 298 K is really *Cmcm*, but that the distortion from *Fmmm* is so slight that the diffraction data necessary to mark the difference between the two groups are so weak as to be unobservable using a conventional diffractometer. This explanation is consistent with the anisotropic displacement parameters observed for the 298 K structures, **1a**, **2a**, and **2c**. The displacement ellipsoids for **2a** are shown in Figure 2a and reveal a systematic extension of the displacements in the same direction, namely perpendicular to the planes of the cyanurate ligands. This is the result that would be expected if a structure that was really *Cmcm* with molecular point symmetry C_{2v} were constrained to *Fmmm* and D_{2h} in the least-squares refinement. It is worth noting that refinement of the 298 K structure **1a** in space group *Cmcm* yielded results qualitatively similar to those derived using *Fmmm*. This result is to be expected, even if the space group were really *Cmcm*, because we have not observed the data necessary to distinguish the slight distortion to *Cmcm* from rigorous *Fmmm* symmetry. It turns out that the magnitude of the distortion of the thermal parameters is also consistent with a critical temperature T_c well above 300 K.[28]

There is a second possible explanation for the elongated displacement ellipsoids of the room-temperature structure. Since there is a first-order component to the phase transition, the rotation of half the ammonia ligands that we observe at and above 223 K, it is possible that the space group is rigorously *Fmmm* at 298 K as a result of deviation from pure second-order behavior. In this case the elongated ellipsoids would represent disorder, probably dynamic, between two molecular congeners of C_{2v} symmetry with opposite directions of distortion. The atomic positions and observed molecular symmetry of D_{2h} would then be *apparent.* The concept of apparent positions and symmetry has been discussed before, mostly in the context of Jahn−Teller effects.[14−16,31]

No matter what the ultimate explanation for the elongated displacement ellipsoids in the room-temperature structure turns out to be, it is beyond doubt that the molecular symmetry remains C_{2v}. This conclusion is supported by the spectroscopic data.

Possible Causal Factors for the Phase Transition. With the available data, we are able to examine three possible causes for the crystal and molecular distortion, and we can cast doubt on at least two of them as the principal source of the distortion at lower temperatures. The question is better put in the converse: What determinative factor of the *Cmcm* structure at low temperature is overcome by thermal energy when the temperature is raised, lowering the polarity of the overall structure and concomitantly of the nickel complex?

The first possibility, that a thermodynamic feature intrinsic to the nickel complex is involved in this phenomenon, can be cast into doubt since the bond lengths within the molecule suffer no significant change across the entire series of analyses presented here. Any internal phenomenon giving rise to such a distortion would be expected to be accompanied by some such change.

A second possibility involves the change in the hydrogen-bonding pattern described in the Results section (Figure 3). However, once the pattern changes, upon going from room temperature to lower temperature, the molecular distortion continues to increase with lower temperature, while the new hydrogen bonds (such as N(4a)−H(41a)···O(4) in Figure 3b) do not change further. So, there is reason to doubt that the hydrogen bonding at the four-molecule junction is the principal cause of the observed phenomenon.

The third factor that can be implicated in the phase transition and consequent molecular shape change is seen in the cyanurate stacking pattern. In the 298 K structure, all of the intermolecular inter-cyanurate spaces are identical and related by crystallographic symmetry. The stacking distance (Table 3) is of the order of 3.64 Å, and the stacked cyanurate rings are nearly eclipsed. The relevant parameters are collected in Table 3, in which "cyan slip distance" refers to the distance that one cyanurate ring would have to travel in its plane in order to be eclipsed with its neighbor. For the 298 K structure, the slip distance is about 0.67 Å in all cases.

In the low-temperature *Cmcm* structure, however, the inter-cyanurate spaces are not equivalent. One of the stacking gaps, that relating a cyanurate at (x,y,z) with one at $(1 - x, -y, 1 - z)$, is somewhat shorter, with values decreasing from 3.476(11) Å at 223 K to 3.354(13) Å at 100 K, and then diminishing

(28) Bürgi, H.-B., private communication, 1998.

(29) Salje, E. K. H. *Acta Crystallogr., Sect. A* **1991**, *A47*, 453−469.

(30) The structural data used in this analysis were from **1c** (100 K), **1b** (150 K), and **3** (223 K). The data from **4** (148 K) were essentially identical to those from **1b**, while **2b** (139 K) was an outlier. The behavior of **2b** can be explained as the result of an impurity of *OC*-6−33-[Ni(cyan-κN)$_2$(NH$_3$)$_2$(H$_2$O)$_2$], which could give rise to exaggerated distortion through cooperativity. We propose that such an impurity was also responsible for the observation of a *Cmcm* structure for [Ni(cyan-κN)$_2$(NH$_3$)$_4$] at room temperature in our previous study of the coordination chemistry of cyanurate. More work is underway on this question.

(31) Stebler, M.; Bürgi, H.-B. *J. Am. Chem. Soc.* **1987**, *109*, 1395−1401.

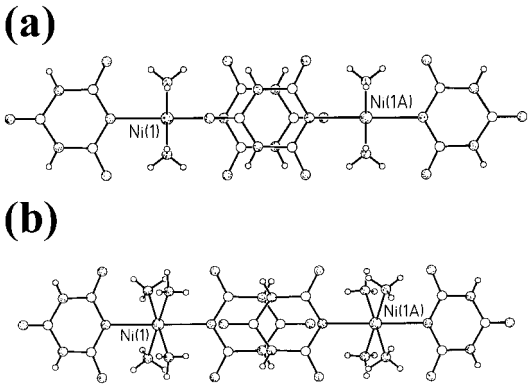

Figure 8. Nonperspective drawings of two molecules of *trans*-[Ni(cyan-κN)$_2$(NH$_3$)$_4$] at (a) 298 K, **2a**, and (b) 100 K, **1c**. The two cyanurate groups at the center of each drawing are parallel to the plane of the paper. The molecule centered at Ni(1) is at *(x,y,z)* in each case, and the molecule containing Ni(1A) is at *(1 − x,1 − y,1 − z).*

to 3.330 Å in the neutron structure at 11−16 K. (This is "cyan stacking distance 2" in Table 3.) This pair of cyanurate ligands remains nearly eclipsed, with slip distances all less than 0.46 Å. The second inter-cyanurate stacking gap, however, undergoes a more pronounced change as the temperature is lowered. This is represented by the parameters "cyan stacking distance 1", and so forth, in Table 3. The distance between the cyanurate at *(x,y,z)* and that at *(1 − x,1 − y,1 − z)* changes from 3.649(10) Å at 223 K to 3.547(13) Å at 100 K. The corresponding slip distance grows monotonically from 1.374 Å at 223 K to 1.76 Å at 100 K and to 1.924 Å at 11−16 K. Figure 8 shows nonperspective drawings of this second cyanurate stacking interaction at two temperatures. The passage from nearly eclipsed to staggered is clearly visible. While we cannot offer positive proof that this is a causal feature in the phase transformation, this stacking interaction does change monotonically with temperature and, in the absence of further evidence, cannot be ruled out as the cause of the phenomenon.

Magnetic Characterization of the Low-Temperature Structural Phase. We will focus the discussion of the magnetism on three different aspects of the magnetic behavior of this compound, which also correspond to three well-differentiated temperature regions. First, in the temperature region between 300 and 100 K, where the structural transition occurs, no magnetic changes are observed. Structural changes can affect the coordination around a magnetic ion and modify its effective spin either through a crossover effect involving the electronic levels or through depopulation of the upper levels of the ZFS. The former can be ruled out in the case of Ni^{2+} ions. With regard to the ZFS, the structural changes in this case mainly affect the disposition of the cyanurate ligands with respect to a central molecular plane and the relative orientation of the NH_3 groups. These changes cause very little modification in the coordination geometry around the Ni^{2+} ions, as supported by the spectroscopic results, and consequently should not affect the ZFS appreciably. The fitting of the Curie−Weiss law to the magnetic data and of the bonding parameters to the electronic spectra indicate that the ZFS is very modest, and thus that changes in the effective spin because of thermal depopulation should arise at much lower temperatures.

Below 50 K the magnitude of the effective moment drops rapidly with temperature due to antiferromagnetic interactions. Since antiferromagnetic ordering of this material arises at 2.61 K, the large majority of these interactions should be short range, and the system should present low dimensional characteristics. It is useful to calculate the ratio between the ordering temperature, T_N, and the temperature at which the maximum of the susceptibility occurs, $T(\chi_{max})$, since this ratio is sensitive to the spatial range of the magnetic interactions.[32] Magnetic systems with this ratio close to unity lack short-range magnetic interactions and should be considered good three-dimensional magnetic systems. The value of 0.58 calculated for the present compound suggests that the interactions propagate in a two-dimensional net. As we discuss below, three-dimensional interactions must be very weak in this system. Their main interest lies in that they might trigger the cooperative transition into a magnetically ordered phase. The susceptibility data can be fitted very well by assuming a square planar arrangement of the moments using high-temperature series expansion for the general spin Heisenberg model[33] in the temperature range from 300 to 10 K. The fitted curve for a value of the exchange constant $J/k_B = -1.06$ K is represented as a solid line in Figure 6. The values of $S = 1$ and $g = 2.15$ have been taken from the fit to the Curie−Weiss law and introduced as constants into the fit. We can investigate this result further by taking into account the position, $\tau_m = k_B T_{max}/|J|S(S+1)$, and height, $\chi_m = \chi_{max}|J|/Ng^2\mu_B{}^2$, of the maximum of the antiferromagnetic susceptibility. The theoretical values for these constants are respectively 2.18(2) and 0.0521(1) for an $S = 1$ square planar Heisenberg model.[33] These values agree very well with the calculated values, $\tau_m = 2.12$ and $\chi_m = 0.047$, using $J/k_B = -1.06$ K and $g = 2.15$. We can therefore conclude that short-range magnetic interactions tend to propagate in a two-dimensional structural section in which each Ni atom has four nearest neighbors in a square planar arrangement.

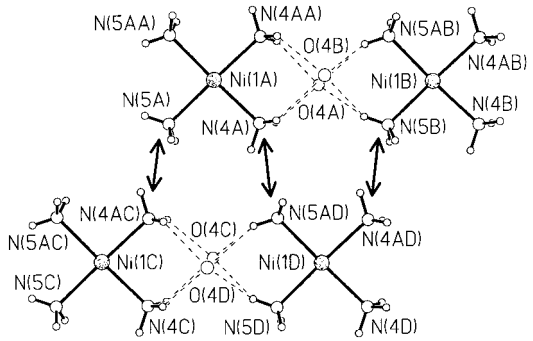

Figure 9. View of one plane parallel to (001) ($z = 0.75$), with magnetic interactions among the Ni atoms. The Ni−N(cyanurate) bond is perpendicular to the plane of the figure. Structural data were taken from **2b**.

We can identify the most likely pathways for the propagation of the magnetic superexchange interactions. Inspection of the structure of the compound at low temperature shows that the Ni atoms occupy positions in (001) crystallographic planes with $z = {}^1/_4$ and $z = {}^3/_4$. These planes also contain the ammine nitrogen atoms and are perpendicular to the Ni−N(cyan) vectors. (The following analysis is based on structure **2b**.) Within each of these planes, each Ni atom has four Ni nearest neighbors (nn) at 7.010 Å and two Ni next-nearest neighbors (nnn) at 7.226 Å, as shown in Figure 9. Interactions between nn Ni atoms, which we shall designate J_{nn}, propagate through Ni−N···N−Ni bridges such as Ni(1A)−(2.066 Å)−N(5A)···(3.194 Å)···N(4AC)−(2.079 Å)−Ni(1C), in which the distances along the propagation chain are given in parentheses. Interactions between nnn Ni atoms, J_{nnn}, propagate through hydrogen bonds along

(32) de Jongh, L. J.; Miedema, A. R. *Adv. Phys.* **1974**, *23*, 1.
(33) Navarro, R. In *Magnetic Properties of Layered Transition Metal Compounds*; de Jongh, L. J., Ed.; Kluwer Acad. Publ.: Dordrecht, The Netherlands, 1990; p 105.

double bridges Ni−N−H···O···H−N−Ni, which include more diamagnetic atoms than do the nn pathways. With reference to Figure 9, the interaction pathways between Ni(1C) and Ni(1D) would consist of two equivalent bridges such as Ni(1C)−(2.079 Å)−N(4AC)−(0.83 Å)−H···(2.304 Å)···O(4C)···(2.538 Å)···H−(0.83 Å)−N(5AD)−(2.066 Å)−Ni(1D). Since magnetic interactions depend strongly on distance, as r^{-11} or more,[34] and given the number of intermediary diamagnetic atoms involved in each interaction pathway, we can conclude that $J_{nn} \gg J_{nnn}$, so that the number of neighbors interacting significantly with each Ni is four, namely the Ni nearest neighbors, in good agreement with the theoretical model used to fit the susceptibility data. Interactions between Ni atoms of neighboring planes, which we shall call J_z, require still longer pathways. The distance between adjacent planes of this family is 7.883 Å, and the minimum distance between Ni atoms from neighboring planes is 9.205 Å. Superexchange interactions in this third dimension propagate through pathways that involve atoms from cyanurate groups, such as Ni−N−C═O···H−N−C−N−Ni. We estimate that $J_z < J_{nnn}$.

Below 10 K the square planar Heisenberg model cannot fit the experimental data. One reason for this is that high-temperature series expansions cannot approximate the maximum of the susceptibility very closely without the use of extrapolation techniques such as Padé approximations. Moreover, magnetic ordering of the system arises, and this cannot occur in a two-dimensional Heisenberg model. Two possible mechanisms can be imputed in the magnetic ordering of the compound. First, magnetic interactions between Ni atoms from different planes start playing a role in the interaction Hamiltonian. Although these interactions are very weak, their importance is that they break the symmetry of the two-dimensional Heisenberg Hamiltonian, so that magnetic ordering is possible at finite temperatures. The second possibility is the presence of magnetic anisotropy. Although the Ni^{2+} ions in this compound should be rather isotropic, ZFS can substantially increase the spin anisotropy. We estimate that it is in this temperature region that the depopulation of ZFS excited states becomes important. Therefore, irrespective of the presence of weak magnetic interactions between Ni atoms of neighboring planes, we believe that spin anisotropy is the most likely trigger for the magnetic ordering of the compound at low temperatures.

Conclusions

The unusual behavior presented by *trans*-[Ni(cyan-κN)$_2$-(NH_3)$_4$] in the solid state is, to our knowledge, unprecedented in molecular coordination chemistry. The structural changes that we observe are characteristic of second-order phase transformations, which display smooth variations of distortion parameters with respect to some thermodynamic variable such as temperature. This system thus represents a coupling of a molecule to its solid in such a way that the properties of the solid as a whole lead to significant changes in the molecule, in this case in its shape and electronic transitions. Seen from a perspective emphasizing the extended solid, the molecule serves as a delivery agent for the components of the aggregate structures that exist in the solid—the cyanurate ribbon, the four-molecule junction, and the cyanurate stack—and which in the end must be responsible for the shape changes suffered by the molecule once it is trapped in the crystal.

Such a system provides an opportunity to study a transition-metal center spectroscopically in a continuously changing ligand field, and conversely the nickel center acts as a probe into the shape of the molecule at any given temperature. The observation of a transition-metal center capable of serving as a shape gauge for this thermomorphic crystal-trapped molecule demonstrates the potential utility of coordination chemistry with polyfunctional ligands.

The magnetic properties of *trans*-[Ni(cyan-κN)$_2$(NH_3)$_4$] show that it has interest beyond its thermomorphism. In the paramagnetic region the system displays two-dimensional magnetic interaction, and the magnetic data fit well to a square planar Heisenberg model, permitting the identification of the structural features through which the magnetic interactions are propagated. At very low temperatures the system undergoes a magnetic phase transition and orders as an antiferromagnet at 2.61 K.

Acknowledgment. We thank Prof. Juan Forniés for invaluable logistical support. Funding from the Directorate General for Higher Education (Spain) under Grant PB95-0792 and from the materials program of the C.I.C.Y T. (Spain) under Grant MAT97-951 is gratefully acknowledged. Financial support from the Australian Research Commission was received by M.A.H. Work at Argonne National Laboratory was supported by the U.S. Department of Energy, Office of Basic Energy Sciences, Division of Materials Sciences, under Contract No. W-31-109-ENG-38.

Supporting Information Available: Tables of crystal data, atomic coordinates, bond distances and angles, anisotropic displacement parameters, principal mean-square displacements, and hydrogen atom coordinates for all of the structure determinations (PDF). The structural results are also available in CIF format. This material is available free of charge via the Internet at http://pubs.acs.org.

JA983247T

(34) Palacio, F.; Morón, M. C. In *Research Frontiers in Magnetochemistry*; O'Connor, C., Ed.; World Scientific Publ.: Singapore, 1993; pp 227−281.